RADIOTRONICS

IN THIS ISSUE

Whilst numerous articles are avail-
able on the phenomenon of second
breakdown from the point of view
of explaining the mechanism, this
article attempts to assist the user
in establishing safe operating areas.

These two chapters on tunnel diodes
conclude the series, which is rounded
off by the addition of a list of
definitions on page 71. See also the
message on page 72.

3

CHARACTERIZATION OF SECOND BREAKDOWN

IN SILICON POWER TRANSISTORS

By: Z. F. CHANG and C. R. TURNER*

Introduction

Numerous articles [1,2,3,4,5,6] have been written on second breakdown in transistors. The aim of these articles, which have dealt primarily with germanium transistors, has been to explain the second breakdown phenomenon. In contrast to these articles, this application note has a three-fold purpose: 1) to indicate the degree or severity of second breakdown ($S/_b$) as a function of transistor current handling capabilities and frequency response for RCA silicon power transistors and to compare single and triple diffused devices; 2) to establish safe operating regions and to determine the variation of $S/_b$ with parameters such as voltage, current, time, pulse conditions, etc. for specific RCA triple-diffused power transistors and 3) to develop a $S/_b$ figure of merit to provide an objective comparison between transistor types for use in specific applications.

Second Breakdown (S/$_b$)

In general, second breakdown in a junction transistor is a condition in which the output impedance changes instantaneously from a large positive value to a negative value, then to a final small positive value (see Figure 1). In some respects the $S/_b$ appears similar to a normal avalanche breakdown — either collector-to-base (BV_{CBO}), or collector-to-emitter ($V_{CE(sus)}$). Its two major differences are: 1) $S/_b$ final limiting voltage is always in the 5 to 30 volt range, whereas BV_{CBO} and $V_{CE(sus)}$ usually have much higher limiting values and 2) $S/_b$ is energy dependent
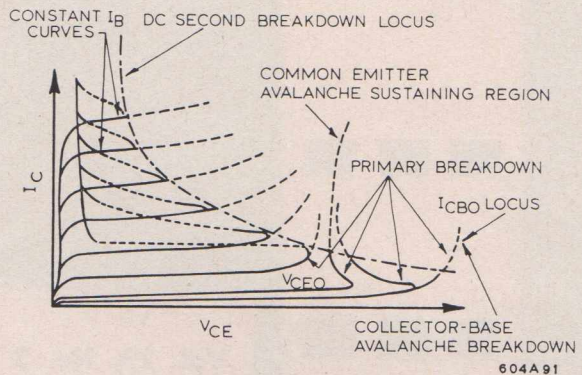
Fig. 1—Transistor Collector Characteristics.

(varies with V, I, T) while BV_{CBO} and V_{CE} are independent of energy to a first order approximation.

Physically, $S/_b$ is a local thermal runaway effect induced by severe current concentrations. These concentrations can result from biasing conditions, excessive transverse base fields and defects in the base region and/or junctions.

Second breakdown can be found in some degree in all junction transistors. However, in many transistor types, primarily small signal and low frequency power versions, the maximum steady state dissipation rating limits the voltage-current product to something less than the critical value necessary to produce $S/_b$. As will be seen from
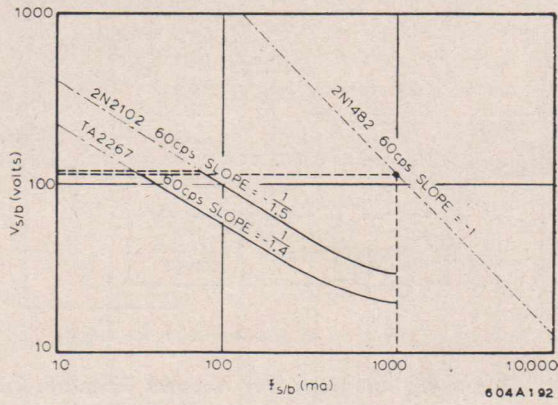
Fig. 2—Critical voltage-current locus to produce S/b, 1 ampere types 2N1482, TN2102, TA2267.
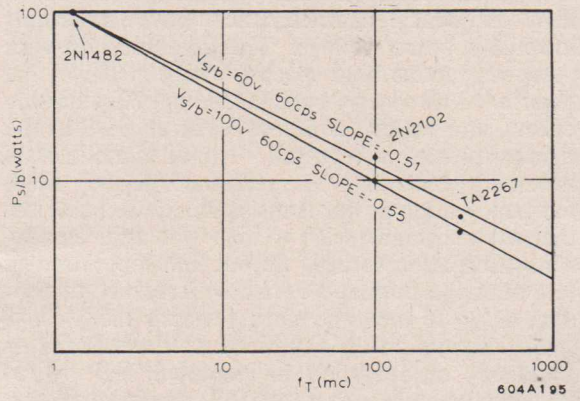
Fig. 5—Critical power for second breakdown versus frequency, 1 ampere types (0.5 a f_T).
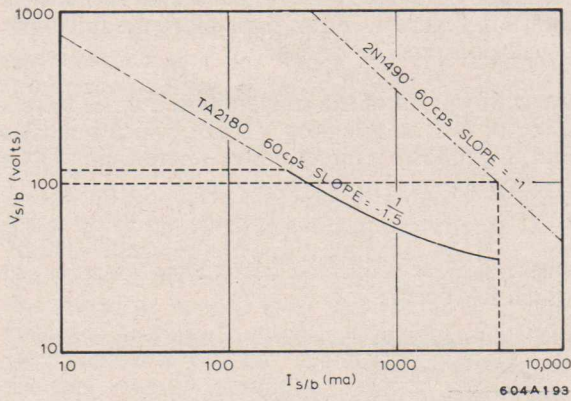
Fig. 3—Critical voltage-current locus to produce S/b, 4 ampere types 2N1490, TA2180.
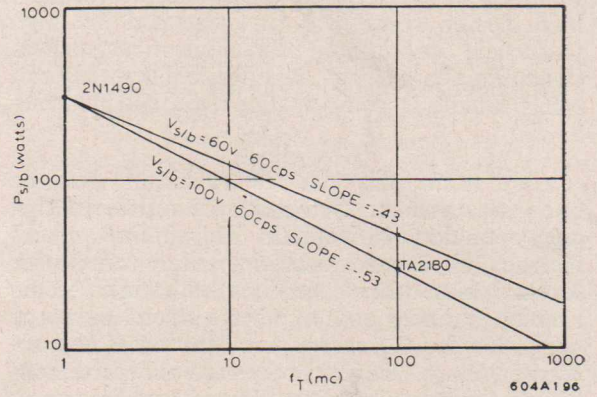
Fig. 6—Critical power for second breakdown versus frequency, 4 ampere types (0.5 a f_T).
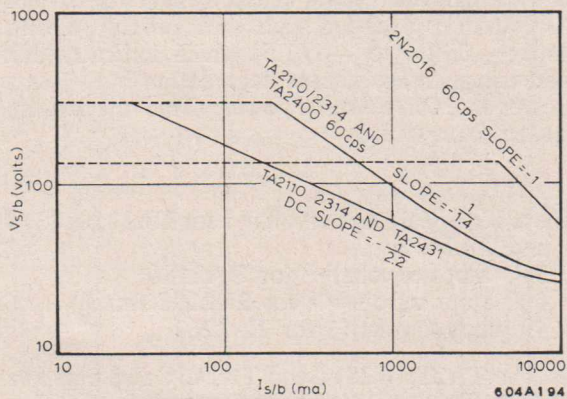
Fig. 4—Critical voltage-current locus to produce S/b, 10 ampere types 2N2016, TA2110/2314, TA2431.
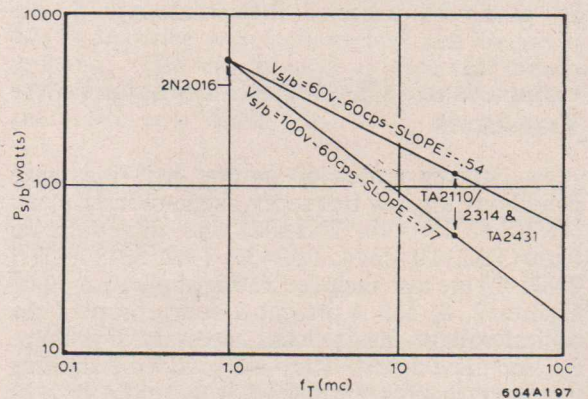
Fig. 7—Critical power for second breakdown versus frequency, 10 ampere types (2.0 a f_T).

data to be presented later, transistors with better high frequency characteristics have invariably lower S/$_b$ power ratings. This is associated with narrower, active base spacing which increases the severity of transverse base fields, amplifies biasing effects, and raises the defect levels relative to the tighter tolerances required. All of these factors adversely affect S/$_b$ as mentioned above. High frequency, high power transistors, which have low thermal resistance with a high potential steady-state dissipation ratings, do not limit operation to less than the critical VI values necessary to produce S/$_b$. If the time during which the steady-state dissipation is applied is decreased, or frequency of operation is increased, the critical VI values necessary to produce S/$_b$ become greater. This change results from the fact that the rate of localized heating is governed not only by the current concentration, but by the thermal mass of the semiconductor material as well, provided that the duration of the instantaneous dissipation is not large when compared to the thermal time constant of the material. Therefore, if high frequency, high power transistors are operated at high frequencies and in nonlinear applications such as switching, Class C, etc., it is possible that they can safely handle large dissipations without incurring S/$_b$.

As a result, this class of transistors must be rated in a manner such that safe reliable design and operation is insured. This rating should include: a) a safe operating range curve for forward bias drive conditions with time as the running variable and b) a safe operating range curve showing S/$_b$ energy as a function of reverse-biased voltage. Curves of forward bias drive conditions for the RCA triple-diffused high frequency power types are included in this application note.

Experiments conducted at ambient temperatures up to 150°C showed that S/$_b$ of some transistors improved while others degraded. Because the results were inconsistent, effect of temperature on S/$_b$ cannot be presented at this time.

Comparison of S/$_b$ for RCA Silicon Power Transistors

S/$_b$ studies under 60 cycles, half-sine wave conditions for low frequency single-diffused types (2N2016, 2N1490, 2N1482) and triple-diffused types (TA2110/2314, TA2431, TA2180, TA2267 2N2102) are also included in this application note. Figures 2, 3, and 4 present a comparison of the critical voltage-current locus necessary to produce S/$_b$ for these types. They are grouped according to current handling capabilities to permit ease of comparison. This grouping is also used for ease of comparison of the critical VI product necessary to produce S/$_b$ versus frequency response plots shown in Figures 5, 6 and 7.

604A198
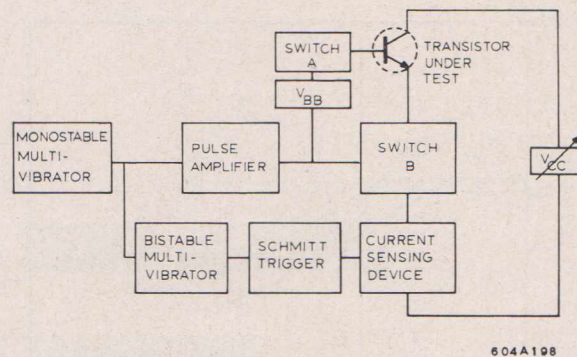
Fig. 8—Block diagram for second breakdown study.

In addition to the critical S/$_b$ plots developed from measurements made at 60 cps, half-sine wave conditions for all transistor types, a plot was developed from measurements made under dc conditions for the TA2110/2314 and TA2431 as shown in Figure 4. From these plots, the following conclusions can be drawn:

1) At 60 cps all of the single-diffused types have a slope of —1 on a log-log VI plot, which indicates that S/$_b$ follows a direct power relationship. This relationship may be expressed as

$$I_{S/b} = KV^{-1} \qquad (1)$$

where $I_{S/b}$ = Collector current (in amperes) at which S/$_b$ occurs.

V = Corresponding collector-to-emitter voltage (in volts)

K = 570 watts for 2N2016 family
330 watts for 2N1490 family
180 watts for 2N1486 family (not shown)
100 watts for 2N1482 family

2) At 60 cps all of the triple-diffused types plot as a straight line except at low voltages (less than 40 volts) on a log-log scale with nearly uniform slope (—1/1.4 to —1/1.5) which indicates that increasing voltage causes degradation in S/$_b$ at a greater rate for constant power. This relationship can be expressed as

$$I_{S/b} = KV^{-1.5} \qquad (2)$$

where K = 860 amps x(volts)$^{1.5}$ for TA2110/2314 and TA2431
310 amps x(volts)$^{1.5}$ for TA2180
100 amps x(volts)$^{1.5}$ for 2N2102 family
49 amps x(volts)$^{1.5}$ for TA2267

3) The TA2110/2314 and TA2431 also plot as a straight line at high voltage dc conditions with a slope of —1/2.2. The equation for this relationship is

$$I_{S/b} = KV^{-2.2} \qquad (3)$$
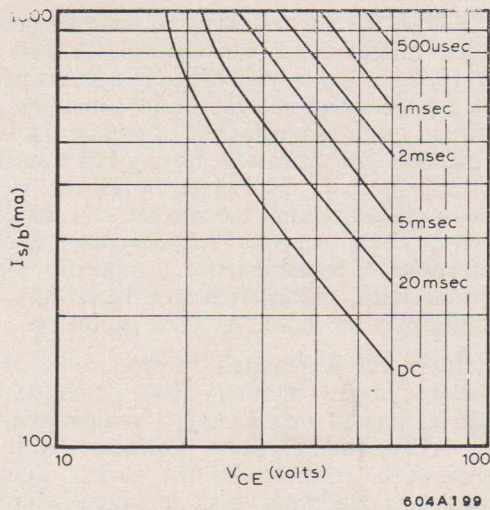
Fig. 9—Safe operating region as a function of pulse width for type 2N2102.

where: K = 7660 amps x(volts)$^{2.2}$ for TA2110/ 2314 and TA2431. Equations (2) and (3) clearly demonstrate that the maximum low frequency power dissipation, if limited by S/$_b$ rather than thermal consideration, has a strong inverse dependence on voltage. Degradation with voltage is the result of a combination of any of the following factors: higher voltage reduces the active base width by spreading the space charge layer, thereby magnifying transverse fields, defects, etc.; for a given current concentration, higher voltage increases the energy level and results in a more localized heating effect; current gain increases with an increase in voltage, thereby accelerating the thermal runaway condition. The dc condition is more severe for S/$_b$ in both magnitude and slope because averaging from the effect of thermal mass is not possible. Pulse duration curves also indicate a change in both magnitude and slope.
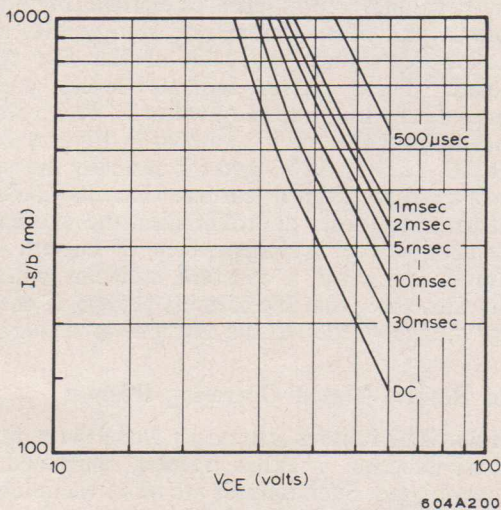
Fig. 10—Safe operating region as a function of pulse width for type TA2267.

Figures 5, 6 and 7 are log-log plots of critical S/$_b$ in terms of power plotted against gain bandwidth product (f$_T$) for the three groups of power transistors. These curves indicate that the higher the frequency response capabilities of a transistor the more severe will be its S/$_b$ limitations. For the case where V S/$_b$ = 60 volts, the resultant straight line plots have an average slope of approximately —0.5. In Figures 6 and 7, a straight line was drawn between only two points. This action is justified in that other available data (not shown in this application note) on competitive types establishes beyond a doubt that a straight line provides the best data average. Additional justification is provided by the straight line obtained when three points in Figure 5 are connected. Using the average slope value results in the following relationship between the critical S/$_b$ power and frequency response

$$P_{S/b} = Kf_T^{-0.5} \qquad (4)$$

where: $P_{S/b}$ = Critical voltage-current product to produce S/$_b$ expressed in watts
f_T = Transistor gain band-width product in the active region, expressed in megacycles
K = 580 watts xMc$^{0.5}$ for 10-ampere types
330 watts xMc$^{0.5}$ for 4-ampere types
115 watts xMc$^{0.5}$ for 1-ampere types

Equation (4) indicates that with present transistor technology a trade must always be made between ability to withstand a given amount of S/$_b$ and frequency performance in selecting transistor types for a given application. It clearly demonstrates that high frequency power transistors should not be used in low frequency applications. Since

$$f_T \propto 1/W^2$$

the S/$_b$ degradation can be explained in terms of narrow base width (W), although no direct correlation between base width and S/$_b$ has been found. Equations (2), (3) and (4) indicate that S/$_b$ is degraded with both voltage and frequency response. This condition is as expected because increasing voltage and frenquency response reduce the active base width.

Testing Conditions and Safe Operating Regions for RCA Triple Diffused Power Transistors

Testing Conditions

The curve tracer method of observing S/$_b$ affords a rapid means of comparing the VI characteristics of transistors when S/$_b$ is triggered. When the transistor has reached its S/$_b$, the last two or three base steps of the collector characteristics are usually so fanned out that it becomes difficult to determine I$_{s/b}$ and the corresponding V$_{CE}$ with any degree of accuracy. In addition, the

half-wave rectified, 60-cycle sine wave sweep does not permit an accurate study of $S/_b$ from the energy standpoint. Since energy is related to time, the duration of power dissipation in the device must be made variable. The block diagram shown in Figure 8 represents the circuit used in performing this test.

Referring to Figure 8, the monostable multivibrator generates a pulse of controlled width. This pulse, after being amplified, is fed to switch A and switch B to simultaneously turn on the base and collector power supplies for the transistor under test. An oscilloscope is connected across the collector-to-emitter junction to measure V_{CE} and a second scope is placed across a current sampling resistor (not shown in the block diagram) to measure the collector current. A sudden decrease in collector voltage accompanied by an abrupt increase in current signify the occurance of $S/_b$. When $I_s/_b$ exceeds the preset level of the current sensing device, the feed-back circuit immediately cuts off the bias to the test transistor. Therefore, a transistor that "breaks" before the pulse ends will not be subjected to a high $I_s/_b$ throughout the remaining pulse. The transition time or the time that it takes a transistor to reach second breakdown, after this phenomenon is initiated by the proper combination of voltage and current varies among transistor types. Moreover, the manner under which $S/_b$ occurs is also markedly different. Some types show more negative resistance than others prior to second breakdown.
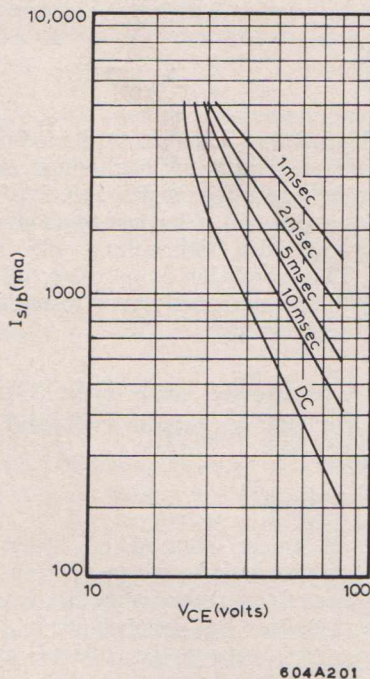
The 2N2102 has a transition time of greater than five microseconds whereas the TA2180 and TA2110/2314 show an extremely fast transition time (less than one microsecond). Since the cut-out circuit has a response time of greater than one microsecond, for transistors having fast transition time, it is necessary to place a resistor in the collector circuit to limit the current to a safe level before the circuit cuts out. Although experimental observations of transition time cannot be related to any electrical characteristics of the devices, this variation may be caused by their geometry.

More power is required to produce $S/_b$ in a device of larger thermal mass, such as the TA2110, than in one having a smaller thermal mass. Also, homogeneity decreases with an increase in the junction size of a device. Because of these two conditions, once localized heating is started, the high current density in a weak point in larger devices can in a much shorter time cause thermal runaway which leads to $S/_b$.

Safe Forward Bias Operating Regions

Figures 9, 10, 11, 12 and 13 define the safe regions for RCA 2N2102, TA2267, TA2180, TA2110/2314 and TA2431 types respectively for the forward bias mode of operation. From these graphs, for a given condition of voltage and current, maximum period of time applied can be determined to insure that the transistor is free from the $S/_b$ region. On most RCA triple-diffused silicon transistors $S/_b$ is controlled at one point under either dc or pulsed condition. Although the rating curves are not fully controlled by factory tests, sufficient derating has been provided to enable them to be used for limit designs under conditions of emitter-base forward bias.

As a more general approach to the rating of transistor $S/_b$, results of the pulse measurements have been analyzed in terms of energy. Figure 14 shows a plot of maximum safe energy level as a function of voltage for each of the five types studied. These curves indicate severe energy degradation with increasing voltage. This voltage effect follows that of $I_s/_b$ shown in Figures 2, 3, 4, 9, 10, 11, 12 and 13 and for basically the same reasons as mentioned earlier. Results indicate that to a first order approximation the maximum safe energy level is independent of current and pulse duration for a constant collector voltage. They also show that the greatest change in energy with voltage occurs in the low power devices.

Safe Reverse-Biased Operating Regions

Transistor failures also occur when the emitter-to-base junction is either opened, shortened, or reverse-biased. Such failures are often encountered in circuits with inductive loads, without the protection of Zener diodes, such as motors, solenoids, relays, deflection yokes, etc. The failures are

604A201

Fig. 11—Safe operating region as a function of pulse width for type TA2180.
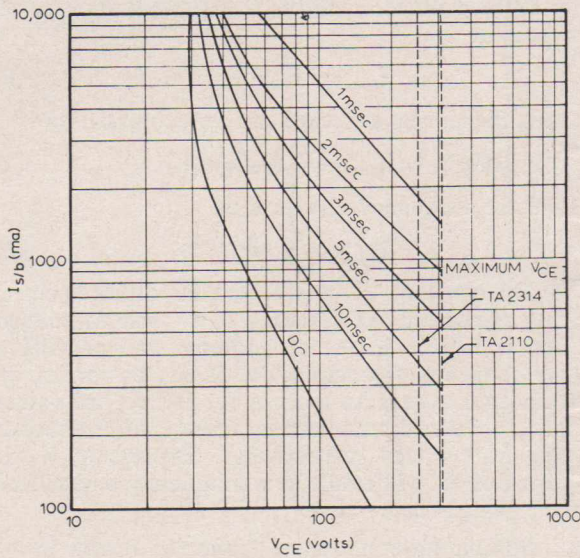
Fig. 12—Safe operating region as a function of pulse width for type TA2110/2314.

commonly attributed to transients or voltage spikes, however, the actual breakdown is $S/_b$ and should be analyzed from the energy standpoint.

Figure 15 illustrates the load line of an inductor with a unit input pulse. This plot is obtained by connecting the horizontal input of an oscilloscope to the collector-to-emitter junction of the tran-
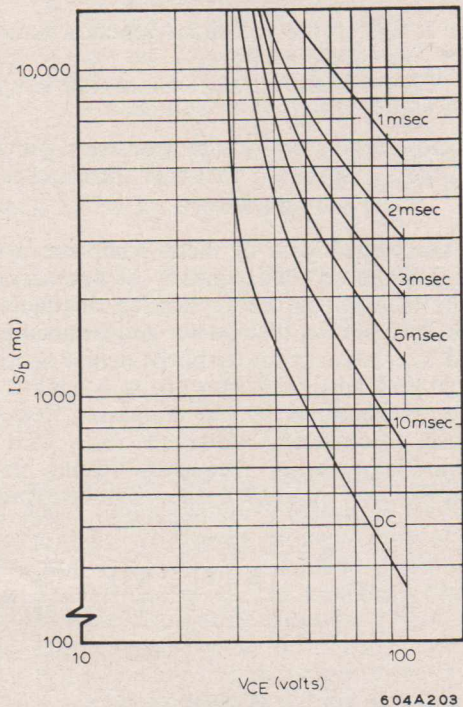
Fig. 13—Safe operating region as a function of pulse width for type TA2431.

sistor, and the vertical input, to the current sampling resistor.

When the drive is turned on, the collector current rises exponentially to a level B determined by the following equation:

$$i = \frac{V_{cc}}{R}\left(1 - e^{\frac{-R}{L}t}\right) \qquad (5)$$

where: V_{cc} = Supply voltage
$\quad$ L $\quad$ = Load Inductance
$\quad$ R $\quad$ = Coil resistance and circuit resistance
$\quad$ t $\quad$ = Input pulse width

The energy storage in inductance L caused by current i is expressed by

$$E = Li^2/2 \text{ (joules)}$$

When the drive is turned off, the inductor tends to discharge its energy through the cut-off transistor resulting in a high voltage across the transistor. When the transient voltage reaches point C, it becomes limited by the transistor sustaining voltage. The low output impedance of the transistor in the sustaining region then provides a discharge path for the stored energy. A plot of $S/_b$ energy versus reverse bias voltages for the RCA TA2110/2314 is shown in Figure 16.
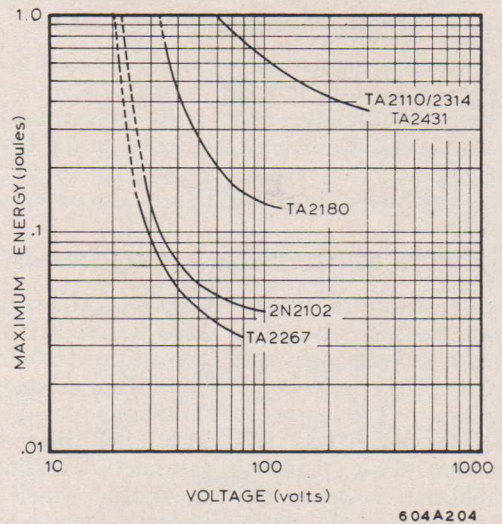
Fig. 14—Maximum safe energy as a function of collector voltage.

Because of the inherent limiting action, it is permissible to have transients which are higher than the transistor avalanche sustaining voltage, provided their energy content is not high enough to cause $S/_b$. The transistor avalanche region varies with the base drive conditions. An associated result of applying a reverse bias is to effectively increase the transistor sustaining voltage. It is not uncommon for the sustaining voltage of a silicon transistor to be increased by more than 50
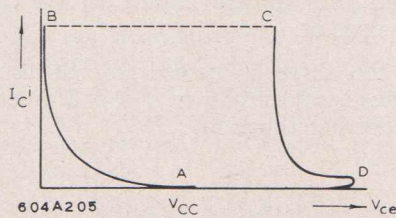
Fig. 15—An inductive load line.

volts as the bias is varied from open to a highly reverse biased condition. Because $I_{s/b}$ decreases with increasing collector-to-emitter voltage, making the transistor more reverse biased results in a lower $I_{s/b}$.

It would be highly desirable to extend the curves of Figures 9, 10, 11, 12 and 13 so that complete safe operating regions for a specific transistor type can be plotted continuously, with the emitter-to-base junction biased from forward to reverse direction. In contrast to the method used to determine the forward safe operating regions, the operating point C with the transistor cut-off is independent of the input pulse duration. The time that the transistor stays in the conducting region (path B →C →D in Figure 15), after the input drive turns off, depends mainly on the switching speed of the transistor and its output impedance under the sustained condition.

In order to induce S/b in a cut-off transistor, energy stored in the inductor is increased either by increasing the supply voltage or the pulse duration. Assuming that the energy dissipated in the circuit is negligible, the energy required to "break" a transistor can be determined from the expression

$S/_b$ Figure of Merit for Power Transistors

All junction transistors exhibit $S/_b$. It has been shown that $S/_b$ becomes more severe with an increase in voltage and transistor frequency response, and less severe with higher frequency operation. The greatest limitations occur for Class A and Class AB linear low frequency operation. Low frequency, saturated switching is not affected because the time during which the transistor is in the high dissipation region is a function of its switching speed. Transistors with the lowest $S/_b$ ratings have the highest switching speeds.

These factors make the establishment of a figure of merit necessary as a common denominator for realistic comparison of $S/_b$ in power transistors. Obviously, any figure of merit must account for both frequency response and frequency of operation. Other important characteristics are the maximum dissipation based on thermal considerations and the constants obtained from the equations relating $S/_b$ to voltage and frequency response, as defined earlier in this report.

If the voltage equation is expressed in general terms as

$$I_{s/b} = K_v V^{-x} \qquad (6)$$

then the power equation can be expressed as

$$P_{s/b} = I_{s/b}V = K_v(V)^{1-x} \qquad (7)$$

and the frequency equation as

$$P_{s/b} = K_f(f_T)^{-0.5} \qquad (8)$$

The constants K_v and K_f are important because they factor out the variation of $S/_b$ due to voltage and transistor frequency response and provide a direct means of comparison of $S/_b$ power for all transistor types. In a sense K_v and K_f are values of $S/_b$ power, normalized by voltage and frequency response values respectively. Expressing K_f in terms of K_v will result in a completely normalized $S/_b$ power expression.

Combining equations (7) and (8) results in

$$K_v(V)^{1-x} = K_f(f_T)^{-0.5} \qquad (9)$$

then solving for K_f yields

$$K_f = K_v(V)^{1-x}\sqrt{f_T} \qquad (10)$$

Normalizing equation (10) by the maximum dissipation (P_{max}) allowed by the thermal considerations of the actual application results in the following equation

$$\frac{K_f}{P_{max}} = \frac{K_v(V)^{1-x}\sqrt{f_T}}{\dfrac{(T_{j\,max} - T_{case})}{R_T}} \qquad (11)$$

where: T_j max is the transistor junction temperature rating

T_{case} is the actual or heat sink temperature

R_T the maximum transistor junction-to-case thermal resistance or derating factor.

To make the figure of merit complete, a term containing the actual frequency of operation (f_o) must be included in the application. Because $S/_b$ studies have shown that power and frequency are related by a square root term, the actual operating frequency should be expressed as a square root function normalized by the transistor frequency response. Combining equation (11) with the normalized operating frequency results in the desired figure of merit (S_b), which can be expressed as

$$S_b = \frac{K_v(V)^{1-x}\sqrt{f_T}}{\dfrac{T_{j\,max} - T_{case}}{R_T}}\sqrt{\frac{f_o}{f_T}}$$

$$\text{or} \quad S_b = \frac{K_v(V)^{1-x}\sqrt{f_o}}{\dfrac{T_{j\,max} - T_{case}}{R_T}} \qquad (12)$$
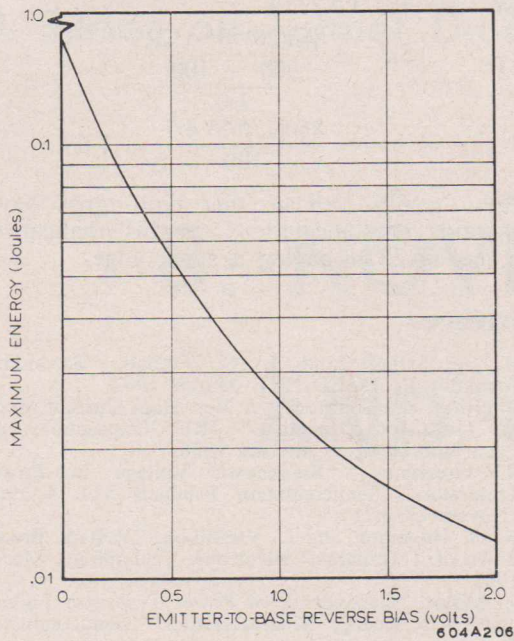
Fig. 16—Maximum safe energy as a function of emitter-to-base reverse bias voltage, type TA2110/2314.

Where: V is the highest collector-to-emitter voltage in volts x is the $S/_b$ index number ($x = 1$ at 60 cps for single-diffused types and 1.5 at 60 cps for triple-diffused types) R_T is junction-to-case thermal resistance or derating factor, expressed in °C/watt f_o is the operating frequency (centre frequency for narrow band amplifiers or lowest frequency for wide band amplifiers.

Note: for Class A biased or dc amplifiers let $f_o = 1 \times 10^{-6}$ and $x = 1$ for single-diffused types and $x = 2.2$ for triple-diffused types.

Equation (11) should be modified for saturated power switching because the critical time is the actual switching time which is related to f_T. The figure or merit for saturated switching becomes

$$S_b{}^1 = \frac{K_v(V)^{1-x} \sqrt{f_T}}{\dfrac{T_{j\,max} - T_{case}}{R_T}} \qquad (13)$$

In determining the transistor type to be used in a given application, consideration should be given initially to voltage ratings, current capabilities and frequency capabilities of the device. Then if a rating for a safe operating region is available (see Figures 9 through 13 for RCA triple-diffused types) make certain that this rating is not being exceeded in the application. Finally, linear equation (12) or switching equation (13) should be used to determine which type has the most desirable $S/_b$ rating for this application.

The type with the most desirable $S/_b$ rating and the higher S_b or S_b value should be selected.

Several practical examples illustrating the use of the second breakdown figure of merit (S_b) are presented below.

Example 1:

Select an RCA transistor type for use in a 20 kilocycle Class C output stage operating with a peak current of 6 amperes at a supply voltage of 32 volts and with a case temperature of 75°C.

Either the 2N2016 (single-diffused) or the TA2314 (triple-diffused) will meet the voltage, frequency and current ratings of this application.

If the following values are substituted in equation 11:

f_o = .020 Mc
$T_{j\,max}$ = 200°C for TA2314 and 2N2016
T_{case} = 75°C
R_T = 1.17°C/W for 2N2016, R_T = 1.0°C/W for TA2314
K_v = 570 for 2N2016, K_v = 860 for TA 2314
x = 1 for 2N2106, x = 1.5 for TA2314
V_{max} = V_{cc} = 32 volts under forward bias condition

and we solve for 2N2016

$$S_b = \frac{\dfrac{570(32)^{°} \sqrt{0\cdot02}}{200 - 75}}{1\cdot17}$$

$$= \frac{\dfrac{570(1)\,(0\cdot14)}{125}}{1\cdot17} = 0\cdot75$$

or we solve for TA2314

$$S_b = \frac{\dfrac{860(32)^{-0\cdot5} \sqrt{0\cdot02}}{200 - 75}}{1\cdot0}$$

$$= \frac{860(1/5\cdot6)\,(0\cdot14)}{125} = 0\cdot17$$

In this particular application, the 2N2016 is operated at a rate which is approximately 5 times more conservative than that for the TA2314, as far as $S/_b$ is concerned. Of course other factors such as better frequency performance and higher primary breakdown ratings favor the TA2314.

Example 2:

Select the optimum RCA transistor for use in a push-pull dc - ac inverter operating at 2 kilocycles. The supply voltage is 28 volts dc and the power output is 150 watts at a case temperature

of 100°C. Here again both the 2N2016 and TA2314 will meet voltage, current, frequency requirements. Because this is a switching application, equation (13) is used. If we substitute the following values

T_{jmax} = 200°C for TA2314 and 2N2016
T_{case} = 100°C
R_T = 1.17°C/W for 2N2016, R_T = 1.0°C/W for TA2314
K_v = 570 for 2N2016, K_v = 860 for TA2314
x = 1 for 2N2106, x = 1.5 for TA2314
V_{max} = V_{cc} = 28V under forward bias conditions
f_T = 0.9 Mc for 2N2016, f_T = 22 Mc for TA2314

and we solve for 2N2016

$$S_b^1 = \frac{\dfrac{570(28)^\circ \sqrt{0.9}}{200 - 100}}{1.17}$$

$$= \frac{\dfrac{(570)(1)(0.95)}{100}}{1.17} = 6.3$$

or we solve for TA2314

$$S_b^1 = \frac{\dfrac{860(28)^{-0.5} \sqrt{22}}{200 - 100}}{1.0}$$

$$= \frac{860(1/5.3)\,4.7}{100} = 7.6$$

These results indicate that both types have outstanding resistance to $S/_b$ in this application with the TA2314 having a slight edge.

References

1. H. A. Schafft and J. C. French, "Secondary Breakdown," PGED, IRE March 1962.
2. Thornton and Simmons, "A New High Current Mode of Transistor Operation," IRE Transactions on Electronic Devices, January 1958.
3. R. Greenburg, "Breakdown Voltage in Power Transistors," Semiconductor Products Vol. 4 1961 (November, p21).
4. F. G. Heymann and L. VanBiljon, "Voltage Breakdown of Transistors," Electronic Technology, March 1962.
5. R. Miller, "Dependence of Power Transistor Failure on Their Energy Characteristics," Semiconductor Products, July 1962.
6. R. Greenburg, "Extending Power Transistor Safe Areas for Fast Switching Pulses," Motorola Application Engineering Report No. 87.

(With acknowledgements to RCA)

NOTICE RE SUBSCRIPTIONS

Readers and intending subscribers are reminded that the subscription rate for this magazine is now £1 (£1/5/- foreign) for 12 issues, and that subscriptions are accepted for multiples of 12 issues if required. Delivery commences with the first issue after receipt of order. Back copies for the current year and previous year may be ordered separately if required; the rate for back copies is 2/6 per copy, post free.

Simple binders intended to hold 12 copies are available at 2/6 each post free, whilst existing stocks last.

Changes of address require one month to become effective, and normally operate on the first issue mailed after receipt of advice. Subscribers are particularly reminded that requests for changes of address should include both the old and the new address; this ensures speedy handling, and protects other subscribers of the same name.

New address stencils now coming into use will carry information regarding the duration of the subscription, allowing readers to check for themselves when their subscriptions are due to terminate. These stencils will be used progressively as renewals are made. The stencil carries a code consisting of two numerals and a letter. The two numerals are the last two figures of the expiry year, whilst the letter shows the last monthly issue due. The letters commence with "a" for January, and go through, omitting "i" and "l", to "n" for December. Thus, for example, code 64j indicates the last copy due to be that for September, 1964. At this date, only a small number of readers have these coded stencils, but it is expected that all will have them shortly.

A Series on Tunnel Diodes

8: NOVEL DEVICES AND CIRCUITS

The **tunnel resistor** is basically a parallel combination of a tunnel diode and a resistor, integrated and miniaturized to fit in the same package as a tunnel diode. The voltage-current characteristic for this device is shown in Fig. 106. The resistor used is a special ultra-low inductance type. The inductance must be kept extremely low to prevent oscillations due to the tunnel-diode negative-resistance region. The flat portion of the resistor characteristic is formed by matching the positive resistance of the resistor to the steepest part of the negative-resistance portion of the tunnel-diode characteristic. The important parameters of the tunnel resistor include the current level of the plateau (high resistance region), the voltage at either end of the plateau, and the degree of flatness of the plateau.
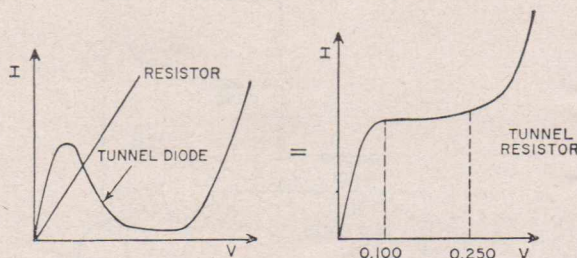
Fig. 106—Tunnel-resistor characteristic.

The tunnel resistor is used primarily as a nonlinear biasing element in tunnel-diode logic circuits, especially in monostable stages. In such applications, tunnel resistors offer faster tunnel-diode recovery time and require less current for
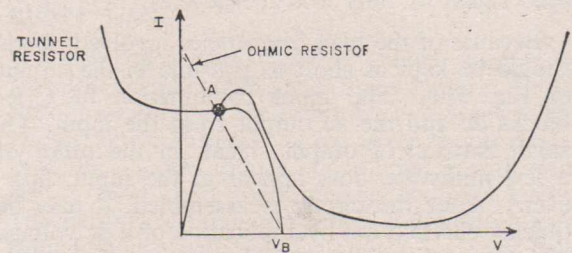
Fig. 107—Tunnel diode having tunnel-resistor load.

triggering a stage than does a purely ohmic resistor. However, the principal advantage of the tunnel resistor is that it reduces the power dissipation. As shown in Fig. 107, the load line of the tunnel resistor is nearly flat at operating point A compared to the dashed line of a conventional resistor using the same bias. As a result, the precise value of the bias voltage has much less effect on the operating current level of tunnel resistors. Thus a simulated constant-current load line can be obtained by use of a tunnel resistor and a low-voltage source, rather than a power-consuming current source. In the case of an ohmic resistor, the same load line at operating point A could only be achieved with a higher voltage source and, hence, a much greater power dissipation.

High-frequency Synchronizer

Many sampling oscilloscopes have inherent bandwidths much greater than the trigger (sync)
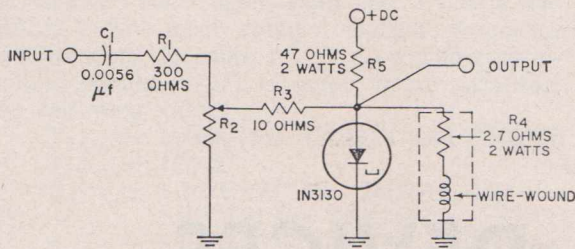
Fig. 108—Tunnel diode synchronizer.

circuits of the scope can handle. For example, although some sampling scopes have a 500-megacycle bandwidth, their trigger circuits cannot sync on frequencies greater than 50 megacycles. Thus, if a 500-megacycle signal is to be displayed, exact subharmonics of the input signal must be generated to trigger the scope sweep circuits. The tunnel diode is the only known device capable of triggering scopes over such a wide frequency range. The simple tunnel-diode counter shown in Fig. 108 can achieve "countdowns" greater than 50 to 1, and can be used at frequencies higher than 500 megacycles. The upper usable limit is not known, but sine waves have been successfully displayed up to 1.2 gigacycles on a sampling scope capable of handling a maximum sync signal of only 100 megacycles.

Because of the high frequencies involved, loads should be kept as short as possible in the circuit of Fig. 108. The input combination of $C_1 R_1$ blocks dc and the ac output from the input. (A small fraction of output signal, in the order of a few millivolts, does appear at the input, however.) After the circuit is assembled, it may be quickly checked out by application of a dc voltage of five to seven volts and observation of the output on a standard 30-megacycle scope. A trapezoidal-shaped wave having a frequency of five to thirty megacycles should be observed.

Operation of the counter is as follows: First, the output is connected directly to the scope trigger input socket, and then the input is connected to the signal source or trigger takeoff. (A

minimum input signal of about ten millivolts is required.) At this point, a dc voltage of approximately five to seven volts is applied, and the voltage, resistor R_2, and the scope trigger controls are slightly adjusted until a stable display appears. These adjustments must be made slowly and very carefully. If the display drifts (becomes unstable), readjustment of the dc voltage is usually the quickest way to make the display stable again.
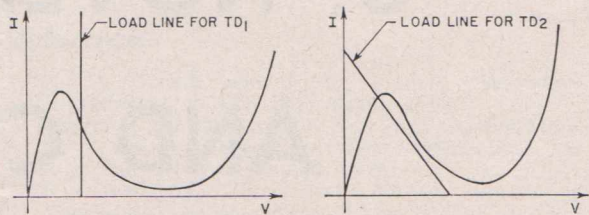
Fig. 110—Tunnel diode load lines.

A more sophisticated synchronizer circuit which can be used at frequencies of more than 3000 megacycles is shown in Fig. 109. In this circuit, TD_1 is a 150-megacycle free-running relaxation oscillator; TD_2 is a monostably biased tunnel diode. The loadlines for these diodes are shown in Fig. 110. The output is at a frequency of approximately 50 to 100 kilocycles. Peak-to-peak voltage up to one volt can be provided at the output by use of a gallium arsenide 50-milli-ampere tunnel diode for TD_2. The input and coupling elements (C_1 and R_3) also may be replaced by high-speed diodes to reduce the feedback of the output into the input. The voltage developed across TD_1 must be held to a maximum of 500 to 600 millivolts; otherwise an input attenuator is needed.

The inductance L_1 must be kept to an extremely low value (approximately 1 to 10 nanohenries) for TD_1 to run freely at more than 100 megacycles. R_1 and R_5 may be one to two ohms.

Fig. 109—Five-gigacycle synchronizer circuit.
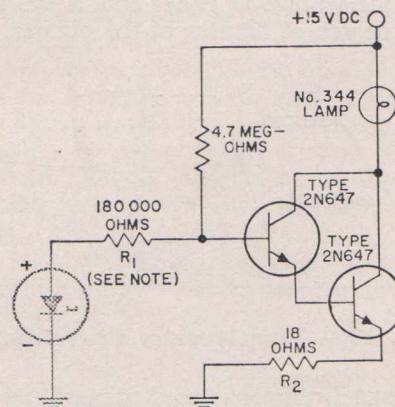
Fig. 111—Tunnel diode indicator for grounded anodes (R_1 should be physically close to the diode).
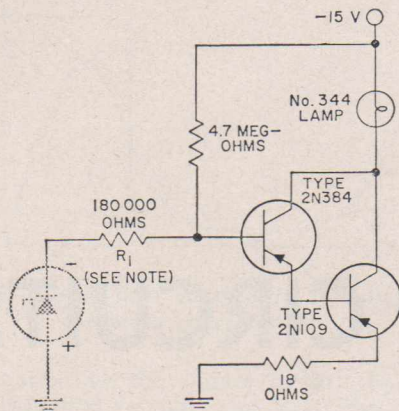
Fig. 112—Tunnel diode indicator for grounded cathodes (R₁ should be physically close to the diode).

Tunnel Diode Indicator

Figs. 111 and 112 show two circuits which can be used to provide a visual indication of whether the tunnel diode is in the high or low state. Because the input impedance of either circuit is greater than 100,000 ohms, negligible current is drawn from the diode under observation.

Scale Expander

A useful circuit which permits tunnel-diode peak current to be measured on a curve tracer with discrimination better than 0.1 per cent and accuracy better than 0.5 per cent is shown in Fig. 113. This simple attachment effectively magnifies the top portion of the tunnel-diode characteristic ten times. Thus, a one per cent current deviation represents one major division instead of one-half of a minor division as on a conventional curve tracer graticule.

This attachment basically expands the range of the vertical-positioning control so that the top portion of the characteristic can be seen on an expanded scale. Calibration is most easily obtained by use of a diode having a known peak current. (This calibration unit may have been measured on the precision-measurement equipment described in the section on Measuring Circuits.) Once the set is calibrated, the vertical-positioning controls must not be disturbed.
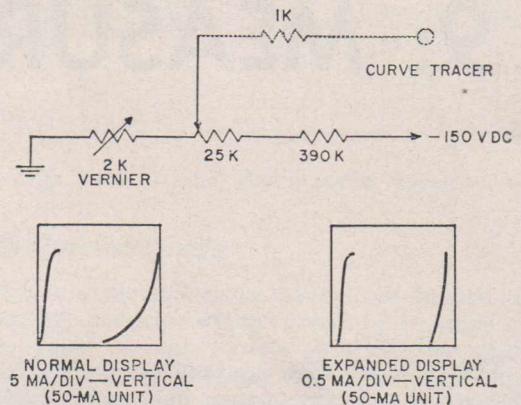
Fig. 113—Scale expander.

Other Uses

Some other novel uses of tunnel diodes are found in decade counters or ring counters. Under certain conditions, for example, a "count-by-10" circuit can be designed by use of ten tunnel diodes in series. Tunnel diodes in conjunction with transistors have been used in ring counters having 100-megacycle repetition rates. Full adders using tunnel diodes with and without transistors have been described in the literature. (See reference in the section on Switching.) The use of tunnel diodes generally permits simpler full-adder circuitry than all-transistorized circuits.

A Series on Tunnel Diodes

9: MEASURING CIRCUITS

TUNNEL-DIODE parameters are easily measured by display of their characteristics on a curve tracer. When a conventional curve tracer is used, a trace similar to that shown in Fig. 114 appears. The negative-resistance portion of the characteristic is not visible because of the speed with which the diode switches from the low-voltage positive-resistance portion of the curve directly to the high-voltage positive-resistance region. The rapid switching occurs because the curve tracer has a total internal series resistance greater than the absolute value of the diode negative resistance. As a result, the diode load line is similar to that shown in Fig. 115, line A. As the sweep current exceeds the peak current (line B) of the diode, the diode immediately switches to its high state.

One of the requirements for display of the complete characteristic is that the total circuit series resistance R_T be less than the absolute value of the tunnel-diode negative resistance R_j, as follows:

$$R_T < | R_j | \qquad (79)$$

When this condition is satisfied, the diode load line is similar to that shown in Fig. 116. In this case, when the curve-tracer sweep current exceeds the peak current, the diode does not switch directly to the high state, but instead travels through the negative-resistance region continuously. However, the curve tracer characteristics such as those shown in Fig. 117. The presence of such "bumps" or "fuzz" in the negative-resistance region indicates that the diode is oscillating as it is swept through this region. This effect can be prevented by use of a total circuit series inductance L_T (including case inductance) which is less than the product of the

Fig. 114—Tunnel-diode characteristic.

total circuit series resistance, the minimum negative resistance of the diode, and the junction capacitance as shown by the following expression[48]:

$$L_T < R_T \times | R |_{Min} \times C_j \qquad (80)$$

Eqs. (79) and (80) represent the two stability conditions that must be met if the complete tunnel-diode characteristic is to be stably displayed.

For low-peak-current units, the circuit shown in Fig. 118 may be used to display the complete characteristic. In this circuit, resistor R_1 serves to bypass the power source so that only the resistance and inductance of resistors R_1 and R_2
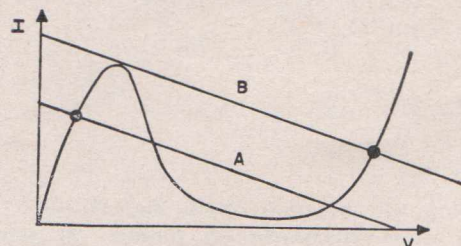
Fig. 115—Tunnel-diode load lines.
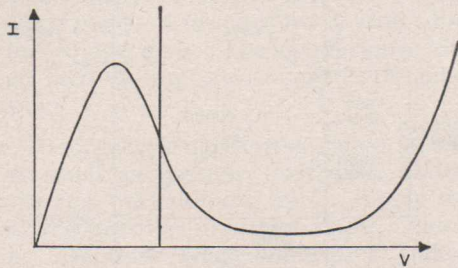
Fig. 116—Load line conditions for display of complete characteristic.

are presented to the tunnel diode. R_2 is the current-sampling resistor, and R_3 is the current-limiting resistor. R_1 and R_2 may be any values as long as their sum is less than $|R_j|$. It is a mistake to assume that the stability of the circuit is increased if R_1 and R_2 are very low. If the resistance $(R_1 + R_2)$ is lower than necessary, it is harder to stabilize the diode, as shown by Eq. (80).

(a)   (b)
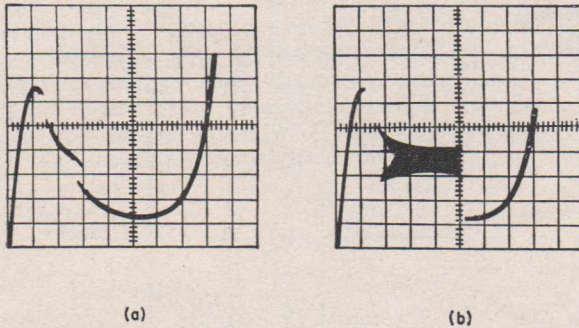
Fig. 117—Presence of imperfections in the diode characteristic.

For medium-peak-current units, the total inductance of two resistors in series may be too large to satisfy Eq. (80). In this case, the circuit shown in Fig. 119 can be used to reduce the circuit inductance by more than 50 per cent.[42] This circuit is basically a form of the familiar Wheatstone bridge. Resistor R_2 is used to obtain a "null" on the bridge without a diode in the circuit. Null is indicated on the scope by a perfectly horizontal line. The diode is then inserted, and the complete curve is traced out. Current through the tunnel diode is measured by the unbalanced condition it causes in the bridge. Methods for the reduction of the inductance of the critical section (R_5 plus tunnel-diode unit) are described in reference 42.

Medium-current units (50 milliamperes or more) generally have too much case inductance to be stabilized completely. For example, a 50-milliampere diode may have a case inductance of 0.4 nanohenry, a negative resistance of two ohms, and a capacitance of 10 picofarads.

Substitution of these values in Eq. (80) produces the following impossible inequality:

$$4 \times 10^{-10} < (2)(2)(10^{-11}) = 0.40 \times 10^{-10}$$
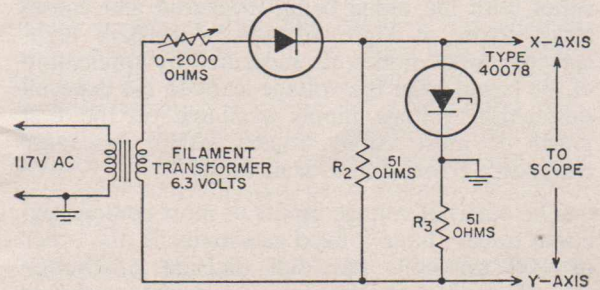
Fig. 118—Tunnel diode curve tracer.

High-Current Units

Most commercial curve tracers are limited to an average collector sweep current of 10 amperes or a peak current of 20 amperes for short durations. Although heavy-duty attachments are available, they are generally quite expensive. Because complicated and costly circuits such as staircase-waveform generators are not needed for the tracing of tunnel-diode curves, a high-current adapter may be easily built at low cost. The adapter shown in Fig. 120 can extend the range of commercial curve tracers to a peak current of approximately 60 amperes. Provided properly rated components are used, this basic circuit can
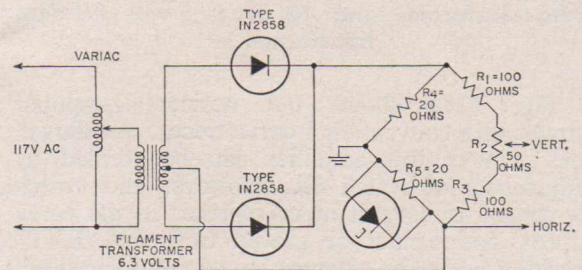
Fig. 119—Tunnel diode curve tracer.

be used to build curve tracers usable up to 1,000 amperes. (Although the transformer specified in Fig. 120 is rated at only 30 amperes, it is possible to trace curves of diodes having peak currents up to 60 amperes because current flows only every half-cycle, and the rms value of a half-rectified sine wave is one-half of the peak current.)

In Fig. 120, two of the four leads connected to the tunnel diode are voltage-sensing leads which measure the voltage appearing directly across the diode. As a result, all voltage drops caused by contact resistance and connecting leads are bypassed. Considerable errors may result in

measurement of peak voltage if the voltage and current leads are not kept separate. Because most commercial curve tracers measure the voltage appearing across their front-panel terminals, any external connecting-lead voltage drop appears in series with the diode being measured and causes large errors at high currents. All RCA high-current tunnel diodes are measured by application of the signal from the voltage leads to the external differential voltage inputs available on the rear panel of most curve tracers. This procedure eliminates errors due to lead drops.

The external voltage inputs of most commercial curve tracers have a fixed sensitivity in the order of 100 millivolts per dial division. Although this scale is not sensitive enough to provide accurate measurement of peak voltage, the horizontal-amplifier section of the circuit can be modified to provide variable gain when the external inputs are used.
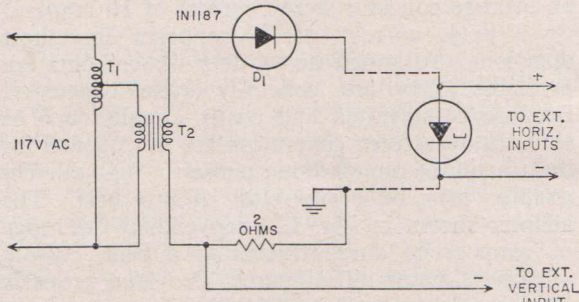
Fig. 120—High-current adapter. (T1 is a variable auto-transformer and T2 is a 5-volt filament transformer.)

Fig. 121a shows the horizontal-amplifier circuit of a conventional curve tracer. As shown, the gain of this amplifier can be verified by adjustment of switch 4R. However, this switch is ganged to several other switches in the curve tracer, and cannot be moved from the "EXT" position when the external inputs are being used. In the modified circuit of Fig. 121b, therefore, switch 4R is bypassed when the external inputs are used, and switch S_1 is added to obtain horizontal sensitivities of 10, 20, 50 or 100 millivolts per dial division.

An important change in the modified circuit of Fig. 121b is the relocation of the 60,000-ohm resistor. If this resistor were to remain in its original location, it would not be connected to the cathode of the valve V354 when S_1 was in the 10, 20, or 50 millivolt per dial division positions. As a result, errors in the order of five per cent might be introduced.

The entire modification described above does not interfere with normal operation of the curve tracer, provided switch S_1 is connected in the
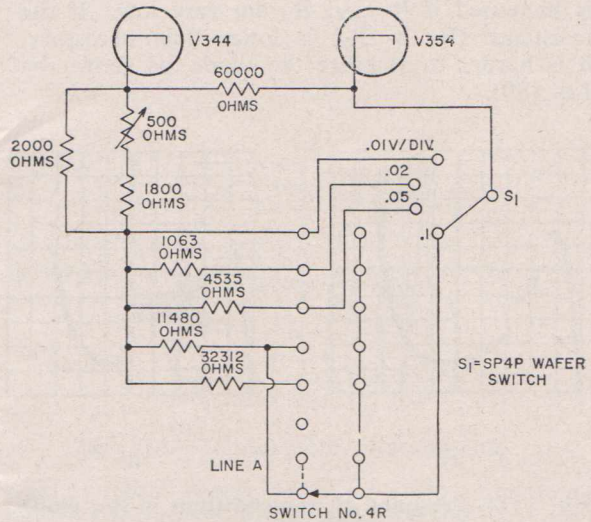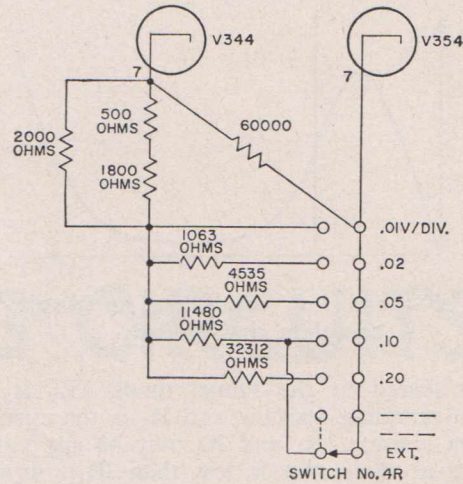
Fig. 121—(a) Simplified circuit for horizontal amplifier switching; (b) modified circuit for horizontal amplifier switching.

0.1 volt per dial division position when the external inputs are not used.

Capacitance

Junction-capacitance measurements at RCA are made on a Wayne Kerr Model B801 admittance bridge, as shown in Fig. 122. Resistor R_1 is used to develop a bias voltage across the tunnel diode. The "unknown" terminals of the bridge appear as a dc short. Capacitance is measured at the valley point with an accuracy of approximately $\pm$ 0.2 picofarad or $\pm$ 2 per cent, whichever is greater.

Operation of the circuit of Fig. 122 is as follows: The power-supply output is increased until the VTVM indicates that the tunnel diode is operating in the valley region. The bridge capacitance dials and the power supply are then

successively adjusted until a null is obtained at the valley point. Capacitance is read directly from the bridge dials. The conductance dial is kept at zero during measurement of junction capacitance.

The 30-megacycle measuring signal should be kept as small as possible, preferably under 10 millivolts rms. In addition, the dc supply should be well regulated to minimize ripple. Shielding may be necessary when high-speed units are measured; otherwise, transients may momentarily push the bias point into the negative-resistance region, thus causing oscillations. The loop inductance (R_1 plus diode socket and corrections) should be made as small as possible.

If it is desired to measure the capacitance of a tunnel diode at points other than in the valley, a rather lengthy procedure must be used. First, the bridge is balanced without any diode in the jig. A shorting strap is then substituted for the diode, and the constant loop impedance is measured. The diode is then inserted, and the admittance of the circuit is measured for various bias voltages. By initial balancing of the bridge at a small positive conductance, the conductance and capacitance in the negative-slope region can be measured, provided the conductance is not too large. From these measurements, the true diode junction capacitance can be computed by means of the following equations:

accuracy on a curve tracer is almost impossible even if perfect calibration is assumed. Because RCA produces tunnel diodes having a ± 1-percent tolerance on peak current, a method more accurate than that of the curve tracer is necessary. This required accuracy is provided by the circuit shown in Fig. 124a. This method was selected for several reasons: (1.) the diode can be stably biased at the peak, (2.) the circuit is not transient or noise-sensitive; (3.) the use of a digital voltmeter for display of the measured parameter reduces the chances of operator error; and, (4.) both peak current and peak voltage are easily measured.

Resistors R_1 and R_2 form a low-inductance monostable load-line for the tunnel diode, as shown in Fig. 124b. The amplifier A' senses the voltage across R_2, amplifies it, inverts it, and feeds it back through R_3. The current generated by this process thus cancels out the current originally flowing in R_2. When the voltage across R_2 drops to zero (ideally), all current flowing through the tunnel diode is diverted through precision resistor R_3 to ground. Therefore, when switch S_1 is in the peak-current position, the digital voltmeter monitors the voltage across R_3 and provides a direct indication of diode current. For measurement of peak current, the power-supply voltage is increased until the diode current reaches a maximum peak. Valley current is

$$C_j = \frac{L_T + \dfrac{C_B}{G_B{}^2 + \omega^2 C_B{}^2}}{\left(\dfrac{G_B}{G_B{}^2 + \omega^2 C_B{}^2} - R_T\right)^2 + \omega^2 \left(L_T + \dfrac{C_B}{G_B{}^2 + \omega^2 C_B{}^2}\right)^2}$$

(81)

$$g_D = \frac{\dfrac{G_B}{G_B{}^2 + \omega^2 C_B{}^2} - R_T}{\left(\dfrac{G_B}{G_B{}^2 + \omega^2 C_B{}^2} - R_T\right)^2 + \omega^2 \left(L_T + \dfrac{C_B}{G_B{}^2 + \omega^2 C_B{}^2}\right)^2}$$

(82)

where C_J is the true junction capacitance, g_D is the diode conductance, $R_T = R_1 + R_S$; $L_T = L_1 + L_S$, and G_B and C_B are values indicated in Fig. 123.

The impedance $Z_1 = R_1 + j\omega L_1$ is the impedance measured when the diode holder is shorted. Fig. 123 shows the variation in capacitance as a function of bias voltage for a five-milliampere tunnel diode.

Precision Measurements

The conventional curve-tracer methods for the measurement of parameters I_P, V_P, I_V, V_V and V_F are simple and rapid, but are not accurate enough for all applications. Better than one per cent

measured by continued increase of power-supply voltage until minimum diode current is obtained. When the switch S_1 is placed in the peak-voltage position, the digital voltmeter B' provides a direct indication of diode voltage. Both peak voltage and valley voltage can then be measured by adjustment of the power supply.

With this circuit, accuracies to 0.1 per cent can be achieved. Short-term repeatability of results is better than ± 0.1 per cent. The sensitivity of the system is sufficient to detect the small changes in tunnel-diode parameters caused by normal variations in room temperature from day to day. Factors affecting accuracy include the tolerance of precision resistor R_3, the voltmeter accuracy, the null voltage across R_2, and the type of jig used to hold the diode.

(a)

(b)

(c)
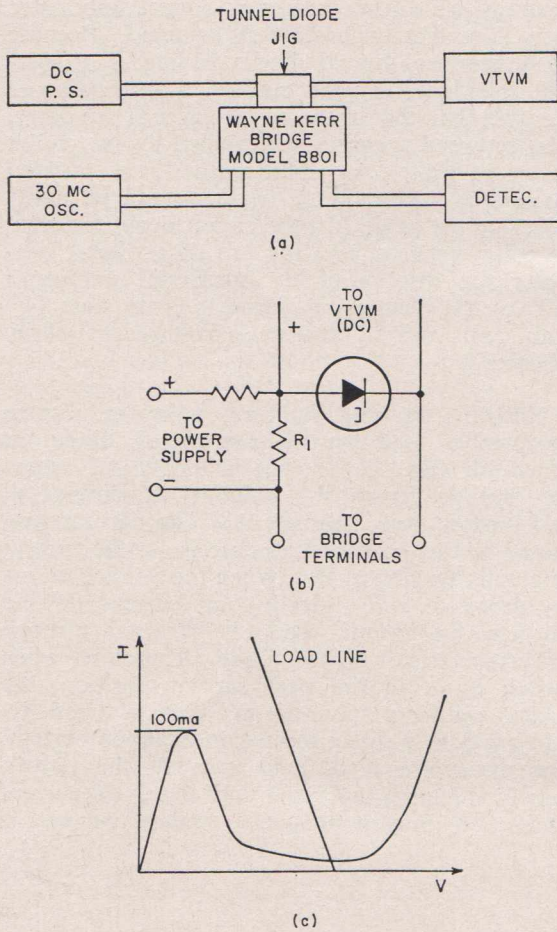
Fig. 122—(a) Block diagram for capacitance test set; (b) tunnel diode jig; and (c) required load line.

In the test circuit shown in Fig. 124a, the precision resistor R_3 has a tolerance of 0.01 per cent. The digital voltmeter B′, which is a four-digit high-speed semiconductor type, has an accuracy of 0.01 per cent. The voltage across resistor R_2, which was measured to be less than 20 millivolts, corresponds to an error of less than 0.04 per cent for a 50-milliampere diode. The possible stray potential differences caused by the contact of two dissimilar metals in the amplifier input leads may be another source of error.

The type of diode holder or jig required depends upon individual needs. A jig for use by circuit design engineers need not be as elaborate as one for production usage. Examples of RCA holding jigs are shown in Fig. 125. Any holder (together with resistors R_1 and R_2) meeting the following requirements is satisfactory, provided R_1 has adequate power-handling capacity. First, the sum of resistances R_1 and R_2 and the tunnel-diode series resistance R_s must be less than the absolute value of the negative resistance, or
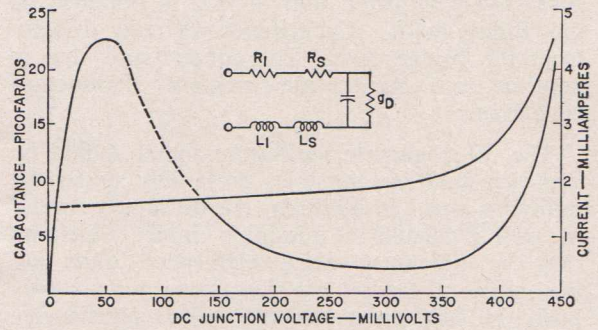
Fig. 123—Capacitance characteristic for five-milliampere tunnel diode.

$$R_T = R_1 + R_2 + R_S \leq |R_j| \qquad (83)$$

Second, the total inductance L_T presented to the diode must be kept below the following limit:

$$L_T \leq R_T \times |R_j| \times (C_j) \qquad (84)$$

Third, the holder for the tunnel diode must not grip the unit in any way which would cause excessive pressure to be applied to the tunneling junction. Finally, the amplifier input leads must be kept separate from the current-carrying leads. If this precaution is not observed, considerable errors may result. For example, it is not permissible to connect the amplifier input lead to point B of Fig. 125a instead of point A.

A′—DC AMPLIFIER
B′—DIGITAL VOLTMETER

(a)

(b)
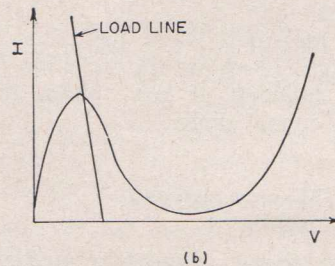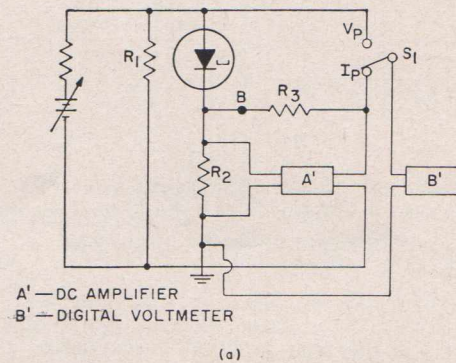
Fig. 124—(a) Precision measurement circuit; and (b) tunnel diode load line.
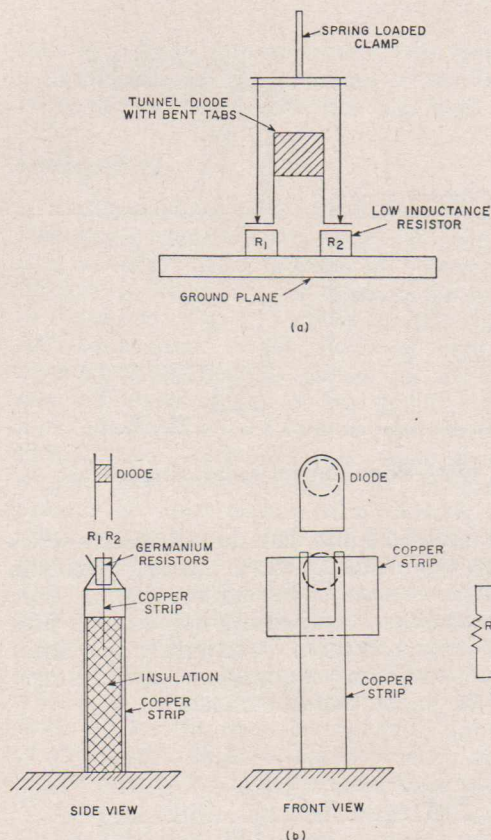
Fig. 125—Typical tunnel diode holders.

The conditions of Eqs. (83) and (84) represent the stability criteria for a tunnel diode. For high-current units, the second requirement is often impossible to meet. However, if the total inductance is kept to an extremely low value, even 50-milliampere low-capacitance units (I_p/C_j greater than or equal to 5:1) can be stabilized slightly past the peak of the diode characteristic.

In both holders shown in Fig. 125, resistors R_1 and R_2 are small cubes of germanium, because conventional carbon resistors are too inductive for this application. However, low-inductance resistors, such as carbon-disc resistors, may also be used in place of the germanium cubes. Both holders accept the RCA tunnel-diode package shown in Fig. 8 in the first section on Theory. The holder in Fig. 125a requires bending of the package tabs; the one shown in Fig. 125b receives straight tabs.

Although forward voltage could be measured with the test circuit shown in Fig. 124, it is much easier and quicker to measure this parameter with the circuit shown in Fig. 126. This circuit consists of a constant-current supply and a digital voltmeter.

Other Methods of Measuring Peak Current

The method shown in Fig. 127 uses a precision ammeter in series with the tunnel diode. Resistor R_2 stabilizes the diode to prevent switching.

This method is not suitable for high-speed units because the ammeter inductance makes it very difficult to stabilize the unit at the peak. Noise from the power supply, or rf pickup, tends to push the bias point slightly into the negative-resistance region. If the inductance in series with the diode is not small enough to meet the stability requirements, then oscillations occur in the negative-resistance region.
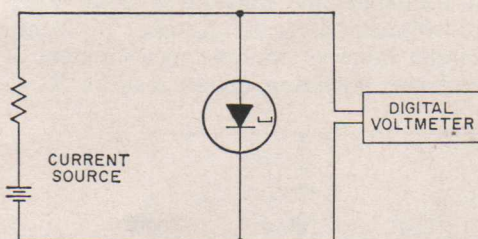
Fig. 126—Forward-voltage measuring circuit.

Fig. 128 shows another method for measuring peak current. In this method pulses of current are used to switch the diode. The peak current equals the pulse current (ideally) when the pulse current is increased until the diode is just barely switching, as observed on the scope. However, there are two disadvantages to this method. First, random noise may switch the diode prematurely, and secondly, it is very difficult to measure either peak or valley voltage. In addition to these disadvantages, a method is needed for measuring the input-pulse amplitude to an accuracy of ±0.1 per cent.
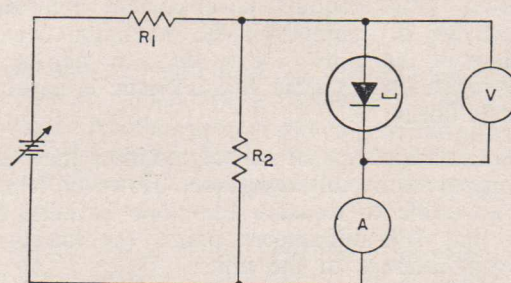
Fig. 127—Peak-current measuring circuit using ammeter in series.

The third method, shown in Fig. 129, is similar to that of Fig. 128 except that a rectified 60-cps sine wave is used to drive the diode past the peak on a load-line. The peak-reading digital voltmeter registers the maximum current passed through the diode (peak current). This method has the same two disadvantages of the method shown in Fig. 128, but offers a rapid method for measuring peak current.

The fourth method, shown in Fig. 130, is similar to the method of Fig. 124a except that the amplifier feedback loop is omitted. In this

circuit, the voltage across resistor R_2 is in direct proportion to the current flowing through the diode. Provided the resistance of R_2 is accurately determined, the peak-current reading may be obtained by "peaking" this voltage. However, it is very difficult to obtain a non-inductive temperature-stable one-ohm resistor having a tolerance of ± 0.1 per cent. It is desirable to use a resistance of exactly one ohm for R_2 and thus avoid a cumbersome conversion factor when the digital voltmeter is read. Another problem with this circuit involves accurate measurement of the low voltage appearing across resistor R_2.
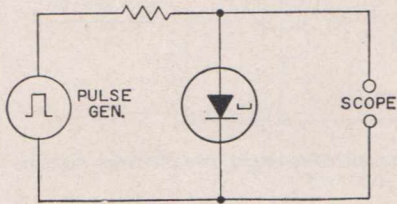
Fig. 128—Peak-current measuring circuit using pulse generator.

Series Resistance

The series resistance of tunnel diodes is normally measured by the curve-tracer method because close accuracy is not required. The tunnel diode is swept out to 200 milliamperes in the reverse direction. The slope of the characteristic between the 100- and 200-milliampere intercepts is considered to be the series resistance for a 50-milliampere unit; lower-peak-current units require lower-current intercepts which are determined by the maximum current ratings of the units ($1.4 \times dc_{max} = ac_{peak}$). In this region, the reverse characteristic is approximately linear.

Series resistance of tunnel rectifiers may also be measured by this technique. However, it may be advisable to measure the slope between the 50- and 100-milliampere points (or lower) to prevent damage to the units.
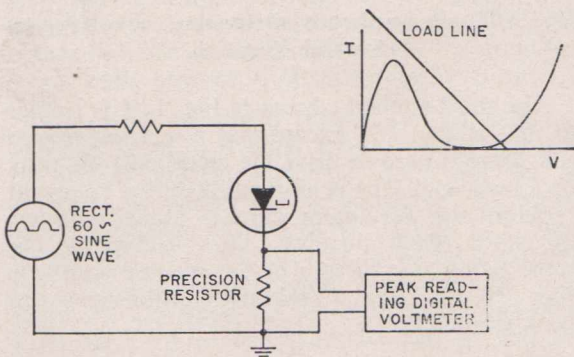
Fig. 129—Peak-current measuring circuit using 60 cps sine wave.
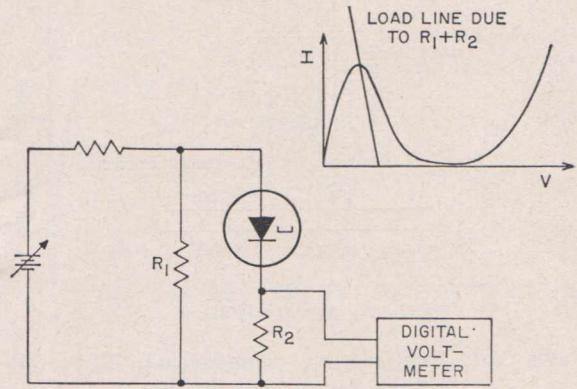
Fig. 130—Peak-current measuring circuit.

Some tunnel-rectifier data do not specify series resistance but instead give a voltage maximum for a given current. This information is more useful in nonlinear (switching) applications than data on series resistance. Conversely, for linear (amplifier, oscillator) applications, series resistance is the more useful parameter.
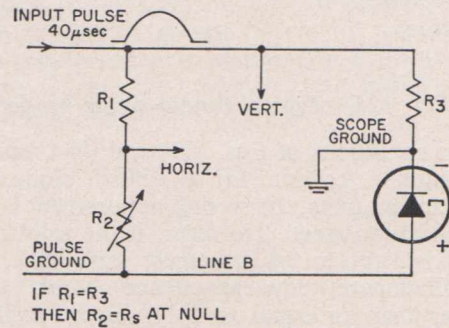
Fig. 131—Series-resistance measuring circuit.

Several other methods for the measurement of series resistance have been proposed. The method shown in Fig. 131 uses the Wheatstone bridge principle.[48] (In this circuit, line B should be grounded and differential scope units used to simulate the scope ground indicated.) The diode is inserted into one arm of the bridge and a pulse is applied to the bridge. When resistor R_2 equals the series resistance at a given bias current, the trace on the scope becomes vertical (perpendicular to the x-axis) at that bias point, as shown by Fig. 132. Because this method tests diodes at larger reverse currents than possible with steady-state methods, the value of series resistance read is lower and closer to the true value than that obtained with the previous method.

Another method is to apply a large pulse of current and a low-level sine wave to the diode simultaneously. The pulse serves to bias the

unit at a large reverse current; the ratio of the superimposed ac-signal voltage to the ac current is the series resistance at this bias level.

Inductance

The inductance of a tunnel diode is a difficult electrical parameter to measure, primarily because it is so small. As a result, it is necessary to use microwave frequencies to measure the inductance of the diode. Fig. 133 shows the test setup used. All connecting cables have a characteristic impedance of 50 ohms, except for the four-ohm line in the dc branch of the circuit. This low-impedance line is used to filter out high-frequency disturbances which may pass down from the rf stages. The variable delay line is adjusted to present an open circuit to rf current from the signal generator. The dc blocking capacitor prevents dc from flowing in the rf signal generator. The VSWR meter is tuned to one kilocycle to pick up the modulating signal generated by the square-wave generator. The dc power supply is used to bias the tunnel diode in its valley region where the junction capacitance of the tunnel diode is known and the dynamic conductance of the tunnel diode is approximately zero.

The inductance is determined from the VSWR of a tunnel diode, the shift away from a short-circuit reference null, and a Smith chart. By means of the equivalent circuit for tunnel diodes, the input impedance Z of the device is found to be

$$Z = R_s + \frac{g_D}{g_D{}^2 + \omega^2 C_j{}^2} + j\left[\omega L_s - \frac{\omega C_j}{g_D{}^2 + \omega^2 C_j{}^2}\right] \qquad (85)$$

Under valley-region bias conditions, g_D becomes approximately zero and Eq. (85) becomes

$$Z = R_s + j\left[\omega L_s - \frac{1}{\omega C_j}\right] = R_s + jX \qquad (86)$$
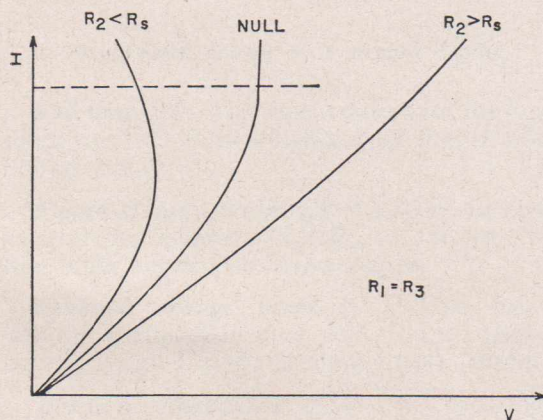
Fig. 132—Oscilloscope display.
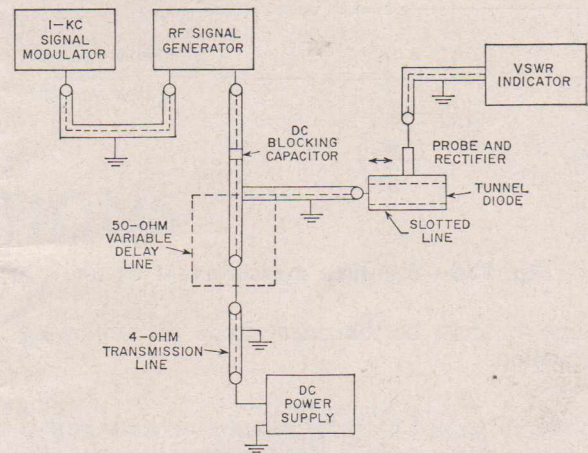
Fig. 133—Test setup for measuring inductance.

The value of X is obtained from the previously mentioned Smith chart. Because the diode capacitance is known accurately in the valley region, the term $1/\omega C_j$ can be computed and added to X to determine ωL_s. When ωL_s is known, L_s can be determined. For the dynamic conductance in the valley to remain essentially zero, a small rf signal must be used to drive the tunnel diode. In these tests, a peak-to-peak amplitude of five millivolts is used. With this signal level, the VSWR indicator must be operated in its most sensitive range. At this sensitivity, the background noise level makes it difficult to locate the null and peak of the standing wave. A typical tunnel diode VSWR is about 32 decibels. Another area of difficulty is the connection of the tunnel diode to the slotted line. The repeatability of measurements is only about 20 per cent.

Typical value of the inductance measured for the RCA standard packages is in the order of 0.4 nanohenry.

Switching Speed

The switching speed, or rise time, of a tunnel diode is directly proportional to the ratio between the peak current I_p and the junction capacitance C_j. This "speed ratio" may vary from about 0.005 to 10.0 or more, depending upon the type of diode. RCA tunneling devices shown in this manual have speed ratios in the range from 0.1 to 10.0 or more. An appropriate "rule of thumb" which relates rise time to the "speed ratio" is that a speed ratio of 0.5 results in a rise time of approximately one nanosecond for a germanium tunnel diode, or two nanoseconds for a gallium arsenide diode. A more accurate estimate of rise
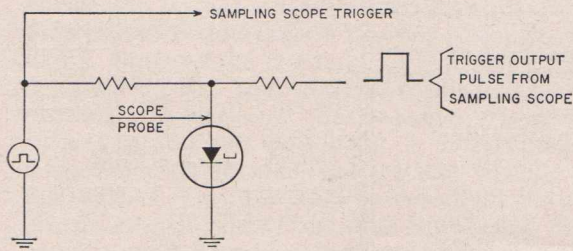
Fig. 134—Rise-time measurement circuit.

VERTICAL: 0.2 V/DIV.
HORIZONTAL: 10 μSEC/DIV.

Fig. 135—Output waveform for ten-ampere tunnel diode operated as a relaxation oscillator.

time t_r may be obtained from the following equation:

$$t_r = C_j \left(\frac{V_F - V_P}{I_P - I_V} \right) \qquad (87)$$

Rise time is generally measured on high-frequency sampling scopes. Conventional scopes lack adequate bandpass, and "traveling-wave" scopes have insufficient vertical (amplitude) sensitivity. A convenient circuit for the measurement of rise times without delay lines is shown in Fig. 134.

An alternate method for measuring rise time, which is quite useful for multiampere units, is to apply a dc dias of approximately 0.2 volt to the diode. At this bias level, the diode automatically begins to operate as a relaxation oscillator, and has a waveform as shown in Fig. 135. The rise time of these pulses closely approximates the rise time obtained by the pulse method (Fig. 134).

Because most commercially available sampling scopes have a maximum response of approximately 0.4 nanosecond, tunnel diodes having a "speed ratio" greater than 1.0 are difficult to measure directly. For this reason, junction capacitance, rather than rise time, is usually specified on tunnel-diode data sheets. When the capacitance is known, the approximate rise time may be computed.

References

48. D. S. Cleverly, "Proposal for the Measurement of Tunnel-Diode Series Resistance", JEDEC Committee, JS-9.
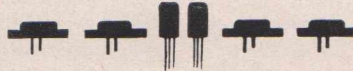
DEFINITIONS

The following terms and symbols are, for the most part, defined with respect to either the tunnel diode characteristic curve or the equivalent circuit shown below.
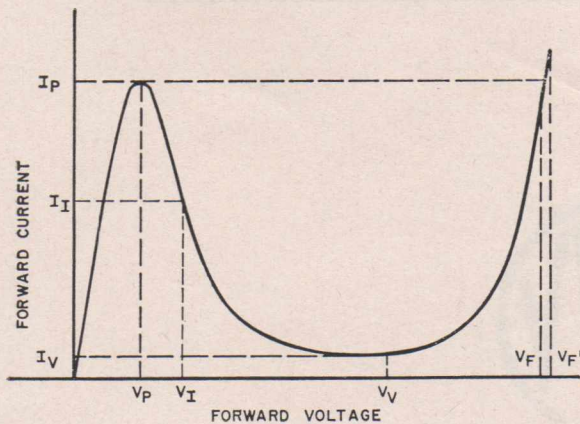
Static forward characteristic of a tunnel diode.
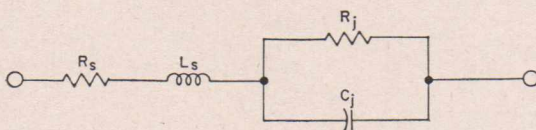
Equivalent circuit of a tunnel diode.

Fall time (t_f)—The time required for the tunnel diode to switch from a high-voltage state to a low-voltage state.

Figure-of-merit frequency (f_c)—The frequency equal to the reciprocal of $2\pi R_{min} C_j$ at a specified bias in the negative-resistance region.

Forward voltage point (V_F')—The forward voltage, greater than peak voltage, for which the current is equal to the maximum peak current.

Junction capacitance (C_j)—The small-signal capacitance associated with the pn junction alone at a specified bias and frequency.

Junction resistance (R_j)—The incremental resistance reduced by the series resistance of the diode, or $dV/dI - R_s$.

Incremental resistance (dV/dI)—The reciprocal of the slope of the current-voltage characteristic.

Inflection point current (I_I)—The current corresponding to the inflection point voltage on the static characteristic curve.

Inflection point voltage (V_I)—The voltage at which the slope of the current-voltage characteristic reaches its most negative value.

Peak current (I_P)—The current at which the slope of the current-voltage characteristic changes from positive to negative as the forward voltage is increased.

Peak voltage (V_P)—The voltage at which the peak current occurs.

Resistive cutoff frequency (f_{ro})—The frequency at which the diode no longer exhibits negative resistance for a specified bias. This frequency is equal to

$$f_{ro} = \frac{1}{2\pi R_j C_j} \sqrt{\frac{R_j}{R_s} - 1}$$

Rise time (t_r)—The time required for the tunnel diode to switch from a low-voltage state to a high-voltage state.

Self-resonant frequency (f_{xo})—The frequency below which the reactance of the diode is capacitive; above this frequency, the reactance is inductive. This frequency is equal to

$$f_{xo} = \frac{1}{2\pi R_j C_j} \sqrt{\frac{R_j^2 C_j}{L_s} - 1}$$

Series inductance (L_s)—The self-inductance of a diode in a specified circuit configuration.

Series resistance (R_s)—That portion of the small-signal terminal resistance of a pn-junction diode which is external to the junction.

Speed index ($I_P : C_j$)—The ratio of the peak current to the junction capacitance. This index determines the speed capability of the device.

Valley current (I_V)—The current at which the slope of the current-voltage characteristic changes from negative to positive as the forward voltage is increased.

Valley voltage (V_V)—The voltage at which valley current occurs.

Publication of this series on Tunnel Diodes has been speeded up over recent months, due to the great interest shown in the series. The whole of this material will shortly be re-issued in book form under the title "TUNNEL DIODES", AWV Publication Number TD1, at 7/6 list, post free.

CLOISTER PRESS (W. SHORT), 45 George Street, Redfern